Mon. Not. R. Astron. Soc. **263**, 861–867 (1993)

Hydrodynamics of relativistic fireballs

Tsvi Piran,[1,2] Amotz Shemi[3] and Ramesh Narayan[1]
[1]*Harvard–Smithsonian Center for Astrophysics, Cambridge, MA 02138, USA*
[2]*Racah Institute for Physics, The Hebrew University, Jerusalem, Israel*
[3]*Department of Physics and Astronomy, Tel Aviv University, Tel Aviv, Israel*

Accepted 1993 February 3. Received 1993 January 29; in original form 1993 January 4

ABSTRACT

Many models of γ-ray bursts involve a fireball, which is an optically thick concentration of radiation energy with a high ratio of energy density to rest mass. We examine analytically and numerically the evolution of a relativistic fireball. We show that, after an early rearrangement phase, most of the matter and energy in the fireball is concentrated within a narrow shell. The shell propagates at nearly the speed of light, with a frozen radial profile, and according to a simple set of scaling laws. The spectrum of the escaping radiation is harder at early times and softer later on. Depending on the initial energy-to-mass ratio, the final outcome of a fireball is either photons with roughly the initial temperature or ultrarelativistic baryons. In the latter case, the energy could be converted back to γ-rays via interaction with surrounding material.

Key words: hydrodynamics – relativity – gamma-rays: bursts.

1 INTRODUCTION

The sudden release of a large quantity of gamma-ray photons into a compact region can lead to an opaque photon–lepton 'fireball' through the production of electron–positron pairs. The term 'fireball' refers here to an opaque radiation plasma whose initial energy is significantly greater than its rest mass. The formation and the evolution of fireballs are of interest in astrophysics (Cavallo & Rees 1978), especially for the understanding of gamma-ray bursts at cosmological distances (Goodman 1986; Paczyński 1986, 1990; Shemi & Piran 1990; Mészaros & Rees 1992, 1993; Narayan, Paczyński & Piran 1992) or in the halo of the Galaxy (Piran & Shemi 1993).

In this paper we investigate the hydrodynamics of fireballs. We begin by summarizing in this section several qualitative results concerning this problem that are already known. Because of the opacity due to pairs, the radiation in a fireball cannot initially escape. Instead, the fireball expands and cools rapidly until the temperature drops below the pair-production threshold and the plasma becomes transparent. In addition to radiation and e^+e^- pairs, astrophysical fireballs may also include some baryonic matter, which may be injected with the original radiation or may be present in an atmosphere surrounding the initial explosion. The electrons associated with this matter increase the opacity, delaying the escape of radiation. More importantly, the baryons are accelerated with the rest of the fireball and convert part of the radiation energy into bulk kinetic energy.

As the fireball evolves, two important transitions take place. One transition corresponds to the change from optically thick to optically thin conditions. As long as the total opacity (pairs + matter) is large, the plasma expands adiabatically as a perfect fluid (Goodman 1986). However, once τ drops below 1, the photons and baryons decouple from each other and continue their evolution independently and without interaction. The second transition corresponds to the switch from radiation-dominated to matter-dominated conditions, i.e. from $\eta > 1$ to $\eta < 1$, where η is the ratio of the radiation energy E to the rest energy M: $\eta \equiv E/Mc^2$ (Cavallo & Rees 1978; Shemi & Piran 1990). In the early radiation-dominated stages, where $\eta > 1$, the fluid accelerates in the process of expansion, reaching relativistic velocities and large Lorentz factors. The kinetic energy also increases proportionately. Later, however, when $\eta < 1$, the fireball becomes matter-dominated and the kinetic energy is comparable to the total initial energy. The fluid therefore coasts with a constant radial speed. The overall outcome of the evolution of a fireball then depends critically on the value of η when τ reaches unity. If $\eta > 1$ when $\tau = 1$, most of the energy comes out as high-energy radiation, whereas if $\eta < 1$ at this stage most of the energy has already been converted into the kinetic energy of the baryons.

The opacity itself has a contribution from electron–positron pairs as well as from electrons associated with the baryons. Initially, when the local temperature T is large, the opacity is dominated by e^+e^- pairs (Goodman 1986). However, this opacity, τ_p, decreases exponentially with

decreasing temperature, and falls to unity when $T = T_p \approx 20$ keV. The matter opacity, τ_b, on the other hand decreases only as R^{-2}, where R is the radius of the fireball. If, at the point where $\tau_p = 1$, τ_b is still > 1, then the final transition to $\tau = 1$ is delayed and occurs at a cooler temperature.

The initial ratio of radiation energy to mass, η_i, determines in what order the above transitions take place. Shemi & Piran (1990) identified four regimes:

(i) $\eta_i > \eta_{pair} = (3\sigma_T^2 E_i a T_p^4 / 4\pi m_p^2 c^4 R_i)^{1/2}$ (where E_i and R_i are the initial energy and radius). In this regime, the effect of the baryons is negligible and the evolution is of a pure photon–lepton fireball. When the temperature reaches T_p, the pair opacity τ_p drops to 1 and $\tau_b \ll 1$. At this point the fireball is radiation-dominated ($\eta > 1$), and so most of the energy escapes as radiation.

(ii) $\eta_{pair} > \eta_i > \eta_b = (3\sigma_T E_i / 8\pi m_p c^2 R_i^2)^{1/3}$. Here, in the late stages, the opacity is dominated by free electrons asociated with the baryons. The comoving temperature therefore decreases far below T_p before τ reaches unity. However, the fireball continues to be radiation-dominated, as in the previous case, and most of the energy still escapes as radiation.

(iii) $\eta_b > \eta_i > 1$. The fireball becomes matter-dominated before it becomes optically thin. Most of the initial energy is therefore converted into the bulk kinetic energy of the baryons, with a final Lorentz factor $\bar{\gamma}_f = \eta_i + 1$.

(iv) $\eta_i < 1$. This is the Newtonian regime. The rest energy exceeds the radiation energy and the expansion never becomes relativistic.

The above summary describes the qualitative features of a roughly homogeneous expanding fireball. In this paper we investigate some aspects of the evolution of an inhomogeneous fireball with a non-uniform radial profile. We show in Section 2 that, after an initial rearrangement phase, the evolution is well described by an asymptotic large-γ solution. The radial profile of the fireball remains frozen over most of this phase, and each streamline follows simple scaling laws as a function of radius. In Section 3 we solve numerically the adiabatic expansion of a spherical fireball and compare the results with the asymptotic solution. We show that the agreement with the theoretical solution is good. Finally, in Section 4 we summarize the results and discuss their implications.

2 SCALING LAWS AND ASYMPTOTIC SOLUTIONS

We consider a spherical fireball with an arbitrary radial distribution of radiation and matter. We discuss here the early phase of evolution, during which the energy and matter densities of the exterior are negligible compared with the internal energy and matter densities of the fireball so that effectively we may consider the fireball to be expanding into a vacuum. In the later stages of the expansion, the matter density in the exterior may be significant and a shock may form. This phase has been discussed by Blandford & McKee (1976, 1977) and Mészáros & Rees (1992, 1993).

The unique feature of a fireball is that initially it is an optically thick system in which the radiation energy dominates the rest mass density. The optical depth is generally due to $\gamma\gamma \to e^+e^-$ and to Compton scattering. Under these conditions there is strong coupling among the photons, and the radiation therefore behaves like a fluid. Furthermore, if baryons are present they will also be strongly coupled to the radiation fluid, and the radiation and matter at each radius will behave like a single fluid, moving with the same velocity. Since the radiation pressure dominates, the pressure p and the energy density e are related by $p = e/3$. Under these conditions, we can rewrite the standard relativistic conservation equations of baryon number and energy momentum (Weinberg 1973) as

$$\frac{\partial}{\partial t}(n\gamma) + \frac{1}{r^2}\frac{\partial}{\partial r}(r^2 n u) = 0, \tag{1}$$

$$\frac{\partial}{\partial t}(e^{3/4}\gamma) + \frac{1}{r^2}\frac{\partial}{\partial r}(r^2 e^{3/4} u) = 0, \tag{2}$$

$$\frac{\partial}{\partial t}\left[\left(n + \frac{4}{3}e\right)\gamma u\right] + \frac{1}{r^2}\frac{\partial}{\partial r}\left[r^2\left(n + \frac{4}{3}e\right)u^2\right] = -\frac{1}{3}\frac{\partial e}{\partial r}, \tag{3}$$

where $\gamma = u^t$, $u = u^r = \sqrt{\gamma^2 - 1}$, and we use units in which $c = 1$ and the mass of the particles $m = 1$. The mass density, n, the total energy density, e (which includes contributions from the radiation as well as from the relativistic electron–positron pairs at temperatures at which the latter are present), and the pressure, p, are measured in the local frame of the fluid, but r and t are in the observer's frame.

If one changes the variables from r, t to r, $s = t - r$, equations (1)–(3) then become

$$\frac{1}{r^2}\frac{\partial}{\partial r}(r^2 n u) = -\frac{\partial}{\partial s}\left(\frac{n}{\gamma + u}\right), \tag{4}$$

$$\frac{1}{r^2}\frac{\partial}{\partial r}(r^2 e^{3/4} u) = -\frac{\partial}{\partial s}\left(\frac{e^{3/4}}{\gamma + u}\right), \tag{5}$$

$$\frac{1}{r^2}\frac{\partial}{\partial r}\left[r^2\left(n + \frac{4}{3}e\right)u^2\right] = -\frac{\partial}{\partial s}\left[\left(n + \frac{4}{3}e\right)\frac{u}{\gamma + u}\right] + \frac{1}{3}\left[\frac{\partial e}{\partial s} - \frac{\partial e}{\partial r}\right], \tag{6}$$

where the derivative $\partial/\partial r$ now refers to constant s, i.e. is calculated along a characteristic moving outwards at the speed of light. After a short acceleration phase, we expect that the motion of a fluid shell will become highly relativistic ($\gamma \gg 1$). If we restrict our attention to the evolution of the fireball from this point on, we may treat γ^{-1} as a small parameter and set $\gamma \approx u$, which is good to order $o(\gamma^{-1})$. Under a wide range of conditions (which we discuss below), the quantities on the right-hand side of equations (4)–(6) are then significantly smaller than those on the left. We therefore set the terms on the right to zero, and obtain the following conservation laws for each fluid shell:

$$r^2 n\gamma = \text{constant}, \qquad r^2 e^{3/4}\gamma = \text{constant},$$

$$r^2\left(n + \frac{4}{3}e\right)\gamma^2 = \text{constant}. \tag{7}$$

Two regimes of behaviour are then immediately apparent. In the radiation-dominated phase ($e \gg n$), we have

$$\gamma \propto r, \qquad n \propto r^{-3}, \qquad e \propto r^{-4}, \qquad T_{obs} \sim \text{constant}, \tag{8}$$

where $T_{\rm obs} \propto \gamma e^{1/4}$ is the temperature of the radiation as seen by an observer at infinity. [Strictly, the radiation temperature depends on $e_{\rm r}$, the energy density of the photon field alone; for $T \ll m_{\rm e}c^2$, $e_{\rm r} = e$, but for $T > m_{\rm e}c^2$, e contains an additional contribution from the electron–positron pairs (see Shemi & Piran 1990); we neglect this complication for simplicity]. The scalings of n and e given in (8) correspond to those of a fluid expanding uniformly in the comoving frame. Indeed, all four scalings in equation (8) were derived for a homogeneous radiation-dominated fireball by Shemi & Piran (1990; see also Goodman 1986) by noting the analogy with an expanding universe. What we have shown here is that the same relations are valid for each individual radial shell in the fireball, even in the more general inhomogeneous case. In fact, these scaling laws also apply to Paczyński's (1986) solution for a steady-state relativistic wind. When we neglect the right-hand sides of equations (4)–(6), the problem becomes effectively only r-dependent.

Although the fluid is approximately homogeneous in its own frame, because of Lorentz contraction it appears as a narrow shell in the observer's frame, with a radial width given by $\Delta r \sim r/\gamma \sim \text{constant} \sim R_{\rm i}$, where $R_{\rm i}$ is the initial radius of the fireball. We can now go back to equations (4)–(6) and set $\partial/\partial s \sim \gamma/r$. We then find that the terms we neglected on the right-hand sides of these equations are smaller than the terms on the left by a factor of $\sim 1/\gamma$. The conservation laws (7) and the scalings (8) are therefore valid so long as the radiation-dominated fireball expands ultrarelativistically with large γ. The only possible exception is in the very outermost layers of the fireball, where the pressure gradient may be extremely steep and $\partial/\partial s$ may be $\gg \gamma/r$. Ignoring this minor deviation, we interpret equation (7) and the constancy of the radial width Δr in the observer's frame to mean that the fireball behaves like a pulse of energy with a frozen radial profile, accelerating outwards at almost the speed of light.

In the alternate matter-dominated regime ($e \ll n$), we obtain from equation (7) the following different set of scalings:

$$\gamma \rightarrow \text{constant}, \qquad n \propto r^{-2}, \qquad e \propto r^{-8/3}, \qquad T_{\rm obs} \propto r^{-2/3}. \quad (9)$$

The modified scalings of n and e arise because the fireball now moves with a constant radial width in the comoving frame. (The steeper fall-off of e with r is a result of the work done by the radiation through tangential expansion.) Moreover, since $e \ll n$, the radiation has no important dynamical effect on the motion and produces no significant radial acceleration. γ therefore remains constant on streamlines, and the fluid coasts with a constant asymptotic radial velocity. Of course, since each shell moves with a velocity that is slightly less than c and that is different from one shell to the next, the frozen-pulse approximation on which equation (7) is based must ultimately break down at some large radius. We consider this question below, but first continue with our investigation of the approximate relations in equation (7).

A scaling solution that is valid in both the radiation-dominated and matter-dominated regimes, as well as in the transition zone between, can be obtained by combining the conserved quantities in equation (7) appropriately. Let t_0 be the time and r_0 be the radius at which a fluid shell in the fireball first becomes ultrarelativistic, with $\gamma \gtrsim$ few. We label the various properties of the shell at this time with the subscript 0, e.g. γ_0, n_0, e_0, and define $\eta = e/n$, $\eta_0 = e_0/n_0$. Defining the auxiliary quantity D, where

$$\frac{1}{D} \equiv \frac{\gamma_0}{\gamma} + \frac{3\gamma_0}{4\eta_0\gamma} - \frac{3}{4\eta_0}, \quad (10)$$

we find that

$$r = r_0 \frac{\gamma_0^{1/2} D^{3/2}}{\gamma^{1/2}}, \qquad n = \frac{n_0}{D^3}, \qquad e = \frac{e_0}{D^4}, \qquad \eta = \frac{\eta_0}{D}. \quad (11)$$

These are parametric relations which give the r, n, e and η of each fluid shell at any time in terms of the γ of the shell at that time. The relation for r in terms of γ is a cubic equation. This can in principle be inverted to yield $\gamma(r)$, and thereby n and e, and η may also be expressed in terms of r.

The parametric solution (11) describes both the radiation-dominated and matter-dominated phases of the fireball within the frozen-pulse approximation. For $\gamma \ll \eta_0\gamma_0$, the first term in equation (10) dominates and we find $D \propto r$, $\gamma \propto r$, recovering the radiation-dominated scalings of equation (8). This regime extends out to a radius of $r \sim \eta_0 r_0$. At larger radii, the first and last terms in (10) become comparable and γ tends to its asymptotic value of $\gamma_{\rm f} = (4\eta_0/3 + 1)\gamma_0$. This is the matter-dominated regime. (The transition occurs when $4e/3 = n$, which happens when $\gamma = \gamma_{\rm f}/2$.) In this regime, $D \propto r^{2/3}$, leading to the scalings in equation (9).

Ultimately, all the energy in the fireball is concentrated in the kinetic energy of the matter, and this determines the value of $\gamma_{\rm f}$. Interestingly, if we write $\gamma_{\rm f}$ in terms of the initial parameters of the fireball at time $t = 0$, we find $\gamma_{\rm f} = \eta_{\rm i} + 1$, whereas when we write it in terms of η_0, γ_0 we have the additional factor of 4/3 as written above. Both formulae represent energy conservation, but the component T^{tt} of the energy momentum tensor behaves differently in the two cases. At time $t = 0$, the fluid is at rest and the radiation energy density is merely e, whereas at $t = t_0$ the fluid is already moving highly relativistically and there is an additional contribution to the energy from the moving pressure, $T^{tt} = \gamma_0^2 e + (1/3)u_0^2 e \sim (4/3)\gamma_0^2 e$.

Let us now return to a consideration of very late times in the matter-dominated phase, at which the frozen-pulse approximation begins to break down. We have already seen that in this phase the radiation density e is much smaller than the matter density n, and also that γ tends to a constant value $\gamma_{\rm f}$ for each shell. We may therefore neglect the term $-(1/3)(\partial e/\partial r)$ in equation (3) and treat γ and u in equations (1)–(3) as constants. We then find that the flow moves strictly along the characteristic, $\beta_{\rm f} t - r = \text{constant}$, so that each fluid shell coasts at a constant radial speed, $\beta_{\rm f} = u_{\rm f}/\gamma_{\rm f}$. Let us label the baryonic shells in the fireball by a Lagrangian coordinate R, moving with a fixed Lorentz factor $\gamma_{\rm f}(R)$, and let $t_{\rm c}$ and $r_{\rm c}$ represent the time and radius at which the coasting phase begins, which correspond essentially to the point at which the fluid makes the transition from being radiation-dominated to matter-dominated. We then find that

$$r(t, R) - r_{\rm c}(R) = \frac{\sqrt{\gamma_{\rm f}^2(R) - 1}}{\gamma_{\rm f}(R)} [t - t_{\rm c}(R)]$$

$$\approx \left[1 - \frac{1}{2\gamma_{\rm f}^2(R)}\right] [t - t_{\rm c}(r)]. \quad (12)$$

The separation between two neighbouring shells separated by a Lagrangian distance ΔR varies during the coasting phase as

$$\left[\frac{\mathrm{d}(\partial r/\partial R)}{\mathrm{d}t}\right]\Delta R=\left[\frac{1}{\gamma_{\mathrm{f}}(R)^3}\frac{\partial\gamma_{\mathrm{f}}}{\partial R}\right]\Delta R. \tag{13}$$

Thus the width of the pulse at time t is

$$\Delta r(t)\approx\Delta r_{\mathrm{c}}+\Delta\gamma_{\mathrm{f}}(t-t_{\mathrm{c}})/\overline{\gamma}_{\mathrm{f}}^3\approx R_{\mathrm{i}}+(t-t_{\mathrm{c}})/\overline{\gamma}_{\mathrm{f}}^2,$$

where $\Delta r_{\mathrm{c}}\sim R_{\mathrm{i}}$ is the width of the fireball when it begins coasting, $\overline{\gamma}_{\mathrm{f}}$ is the mean γ_{f} in the pulse, and $\Delta\gamma_{\mathrm{f}}\sim\overline{\gamma}_{\mathrm{f}}$ is the spread of γ_{f} across the pulse. From this result, we see that there are two separate regimes in the fireball evolution even within the matter-dominated coasting phase. As long as $t-t_{\mathrm{c}}<\overline{\gamma}_{\mathrm{f}}^2R_{\mathrm{i}}$, we have a frozen-coasting phase in which Δr is approximately constant and the frozen-pulse approximation is valid. In this regime, the scalings in equation (9) are satisfied. However, when $t-t_{\mathrm{c}}>\overline{\gamma}_{\mathrm{f}}^2R_{\mathrm{i}}$, the fireball switches to an expanding-coasting phase, where $\Delta r\propto t-t_{\mathrm{c}}$ and the pulse width grows linearly with time. In this regime the scaling of n reverts to $n\propto r^{-3}$, and, if the radiation is still coupled to the matter, $e\propto r^{-4}$.

Independently of the above considerations, at some point during the expansion the fireball will become optically thin and the radiation will decouple. From this stage on, the radiation and the baryons no longer move with the same velocity and the radiation pressure vanishes, leading to a breakdown of equations (2) and (3). The radiation will now coast with a speed exactly equal to c and with a constant radial width. The radiation energy density will clearly scale as $e\propto r^{-2}$. The baryon shells, on the other hand, will coast with their own individual velocities. If the fireball is already in the matter-dominated coasting phase, there will be no change in the propagation of the baryons. If, however, the fireball is in the radiation-dominated phase when it becomes optically thin, then the baryons will continue to be dragged by the photons until the mean path for Compton scattering of an electron by the photons is larger than the size of the fireball. Since this mean free path is smaller by a factor of $(n_{\mathrm{e}}/n_{\gamma})^{1/3}$ than the mean free path for the scattering of a photon by an electron, an additional expansion by a factor of $(n_{\gamma}/n_{\mathrm{e}})^{1/3}$ is required for the baryons to decouple from the radiation (Mészáros, Laguna & Rees 1993). Once this has happened the baryons switch to a coasting phase.

The final outcome of the fireball depends on the stage at which the fireball becomes optically thin. If this happens during the radiation-dominated era, then most of the initial energy will escape as photons, typically with the same temperature as the initial temperature (Goodman 1986). If, on the other hand, the fireball is in the matter-dominated era, then most of the energy will have been converted into the kinetic energy of the baryons and only a negligible fraction will be carried by the photons. However, in this case it is still possible to recover the energy in the form of radiation if the escaping baryons interact with the surrounding matter (Mészáros & Rees 1992, 1993; Blandford & McKee 1977).

3 NUMERICAL RESULTS

We have developed a spherically symmetric relativistic code that follows the evolution of a mass-loaded fireball from an initial configuration at rest, via the acceleration phase, into the asymptotic frozen-pulse regime (Shemi 1993; Shemi & Piran, in preparation). The code is Eulerian and employs a second-order conserved scheme (Bowers & Wilson 1991) which is modified to take into account the extreme relativistic Lorentz factors encountered in this problem. Our scheme is quite different from the one used by Vitello & Salvati (1976), who studied a similar problem. The code has passed several standard tests, including the Richardson test, i.e. the results converge satisfactorily as the grid size is decreased.

The initial profiles for the cases that we present here are

$$e(r,t=0)=\frac{e_0}{(R_{\mathrm{i}}^8+r^8)},\qquad n(r,0)=\frac{e(r,0)}{\eta_{\mathrm{i}}},\qquad \gamma(r,0)=1, \tag{14}$$

where we choose R_{i}, the initial width of the fireball, to be unity. The initial radiation density e_0 is in arbitrary units, and we assume a constant ratio η_{i} of energy to mass. The energy density falls off sufficiently rapidly with radius in the initial profile that the external density is negligible compared to the interior density. We cannot, however, set the exterior density exactly to zero, since this leads to numerical problems. We have explored different initial conditions, and find different pulse shapes, but the overall qualitative behaviour is generally similar to the results described below.

Fig. 1(a) shows a sequence of profiles in the observer's frame of the energy density, γe, and the mass density, γn, for a simulation with $\eta_{\mathrm{i}}=50$. Three phases of evolution are apparent, namely an initial acceleration/rearrangement phase, a short radiation-dominated phase, and a final matter-dominated phase. Conservation of energy requires that, asymptotically, the average Lorentz factor of the expanding fluid should be $\overline{\gamma}_{\mathrm{f}}=\eta_{\mathrm{i}}=1$. We compute $\overline{\gamma}$ at each stage by means of

$$\overline{\gamma}=\frac{\int T^{tt}r^2\,\mathrm{d}r}{\sqrt{(\int T^{tt}r^2\,\mathrm{d}r)^2-(\int T^{tr}r^2\,\mathrm{d}r)^2}}$$

$$=\frac{\int T^{tt}r^2\,\mathrm{d}r}{\sqrt{[\int(T^{tt}+T^{tr})r^2\,\mathrm{d}r][\int(T^{tt}-T^{tr})r^2\,\mathrm{d}r]}}, \tag{15}$$

where the second expression is preferable for numerical accuracy. The average Lorentz factor in this simulation does approach the expected asymptotic value, but it does not quite reach it because we did not let the computation continue for a long enough time.

Early in the evolution, the pulse rearranges itself during a brief acceleration phase. Although with our choice of initial data the ratio between the energy and mass densities, η, initially has a constant value throughout the fireball (equation 14), it changes during this phase and no longer remains constant within the pulse. Generally, η ends up being smaller in the inner parts of the fireball and larger on the outside. This can be seen in Fig. 2, which shows n, e and γ at a fixed moment in time after the end of the early phase of rearrangement. After this phase, the shape of the pulse is frozen and the fireball evolves through a radiation-dominated phase to a matter-dominated state. The transition from radiation-dominated to matter-dominated can be clearly seen in Fig. 1(a), where the matter density is initially lower than the

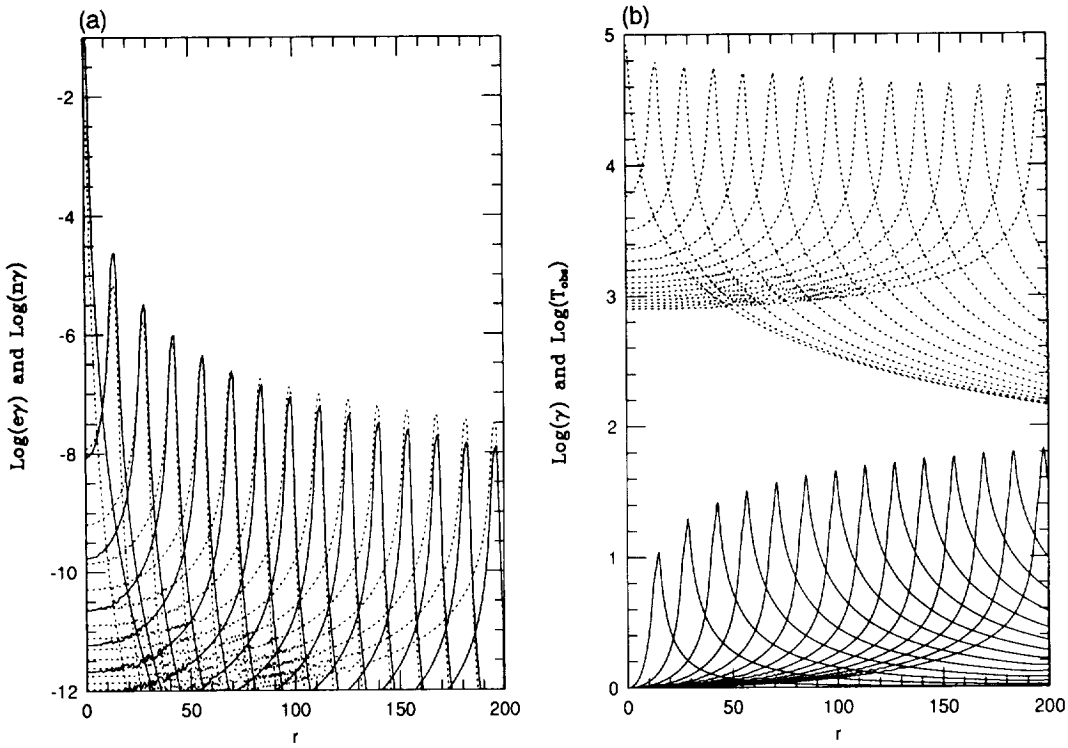

Figure 1. (a) The energy density $e\gamma$ (solid lines) and the mass density $n\gamma$ (dotted lines) in the observer's frame for a numerical simulation in which the initial energy-to-mass ratio $\eta_1 = 50$. (b) The Lorentz factor γ (solid lines) and the observed temperature $T_{\rm obs} = \gamma T = \gamma e^{1/4}$ (dotted lines). The temperature scale is arbitrary.

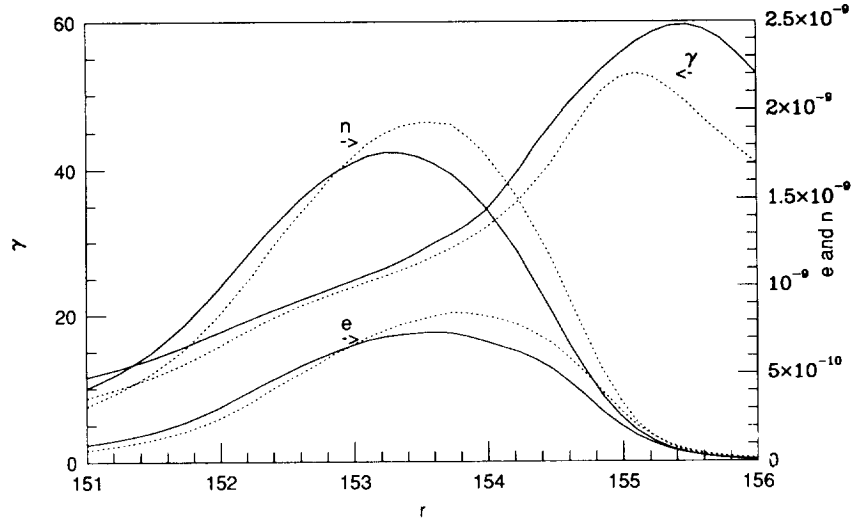

Figure 2. Calculated (solid lines) and extrapolated (dotted lines) n, e and γ profiles at $t = 153.7$ (the end of the computation). The extrapolation is from $t = 14$ (shortly after the end of the rearrangement phase) using equations (10)–(11). The agreement is best in the trailing edge of the pulse in the interior of the fireball, and is less satisfactory in the leading edge. This is a result of the combined effects of the steep pressure gradient and the loss of numerical accuracy at lower densities.

energy density but becomes larger by the end of the computation.

The profile of the Lorentz factor γ at various times in the pulse is shown in Fig. 1(b). We see that γ varies significantly across the pulse. Whereas the mean $\overline{\gamma}_f$ cannot exceed the asymptotic value of $\eta_1 + 1$, the maximum Lorentz factor within the pulse is larger than this and in fact increases throughout the evolution. This happens because the outermost layers of the fireball keep accelerating, as can be seen in Fig. 2. The Lorentz factor therefore peaks ahead of the energy density in a low-density region, and a small fraction of the material is accelerated to these high-γ values. The peak

in γ leads to the highest observed temperature being obtained from the front of the fireball and to lower temperatures being obtained from the interior (Fig. 1b).

In Fig. 2 we compare the calculated pulse at $t = 153.7$ to a pulse extrapolated, using equations (10) and (11), from $t = 14$. The agreement is very good considering that the energy and matter densities have decreased by 4 and 3 orders of magnitude, respectively, while the maximal Lorentz factor has increased by a factor of 6 between these two moments. The agreement is excellent in the inner region of the pulse, but is less satisfactory on the outside. This is partly due to the continuing acceleration of the outer regions, in which the pressure gradient is steepest, and partly because of decreased numerical accuracy in the regions in which the density is very low.

Fig. 1(b) shows profiles of $T_{\rm obs}$, the temperature that would be observed at infinity if the radiation could escape. At early times, there is a drop in $T_{\rm obs}$ due to the broadening of the pulse as a result of internal rearrangement. During the subsequent radiation-dominated phase, $T \propto \gamma^{-1}$ (equation 8), and the observed temperature $T_{\rm obs}$ of each shell remains constant. The overall spectrum of a fireball that becomes optically thin during this phase is a blending of thermal spectra with different temperatures and different blueshifts, and will be slightly broader than a single-temperature thermal spectrum (see Goodman 1986). The spectrum does not change during the radiation-dominated phase, apart from a minor effect due to the addition of a harder component from the acceleration of the outermost layers of the fireball. When a given shell enters the matter-dominated phase, $T_{\rm obs}$ begins to decrease, since T continues to decrease but there is no longer a compensating increase in γ (equation 9). The result is a softer spectrum than that observed during the radiation-dominated phase. The spectrum emitted depends now on the moment at which each shell becomes optically thin. Since different shells become optically thin at different values of γ, we expect the spectrum to be broader than that emitted during the radiation-dominated phase.

The evolution of the relativistic radiation fireball that we have described here and in Section 2 is remarkably different from that of a Newtonian fireball with $\eta_i \ll 1$. Fig. 3 shows the energy density and the mass density for a pulse with $\eta_i = 0.001$. None of the features described earlier appear. Relativistic velocities are never reached and the shape of the pulse is not frozen. We observe instead an expanding, almost homogeneous sphere, rather than an expanding shell of matter and radiation, and the expansion velocity of most of the fireball is roughly the Newtonian velocity $\sqrt{2\eta_i} = 0.045$. A negligible fraction of the matter on the surface is accelerated to higher speeds. Interestingly, the Newtonian fireball bears a strong qualitative resemblance to the relativistic fireball in the local frame. The differences between the two cases arise mainly because of the transformation to the observer's frame. In the Newtonian case, there is no difference between the observer's frame and the matter local frame, but in the relativistic case Lorentz contraction leads to a drastic change in the appearance of the fireball. In the former case the fireball therefore appears to fill the entire sphere of radius r, whereas in the latter case the observer sees a narrow pulse whose width remains of the same order as the original width, leading to a time-scale of $\sim R_i/c$.

4 CONCLUSIONS

We have shown in this paper that fireballs with large initial ratios η_i of radiation energy to rest mass energy show certain common global features during their expansion and evolution. After a short initial acceleration phase, the fluid reaches relativistic velocities, and the energy and mass become concentrated in a radial pulse whose shape remains frozen in the subsequent expansion. The motion is then described by an asymptotic solution (equations 10 and 11; see Section 2), which gives, for each individual shell, scaling laws similar to those of a homogeneous sphere.

The expanding fireball has two basic phases: a radiation-dominated phase and a matter-dominated phase. Initially, during the radiation-dominated phase, the fluid accelerates with $\gamma \propto r$ for each Lagrangian shell. The fireball is roughly homogeneous in its local rest frame but, due to the Lorentz contraction, its width in the observer's frame is $\Delta r \approx R_i$, the initial size of the fireball. When the mean Lorentz factor of the fireball becomes $\bar{\gamma} \approx (\eta_i + 1)/2$, a transition takes place to the matter-dominated phase. Ultimately, all the energy becomes concentrated in the kinetic energy of the matter, and the matter coasts asymptotically with a final Lorentz factor of $\bar{\gamma}_f \approx (\eta_i + 1)$. The matter-dominated phase is itself further divided into two subphases. At first, there is a frozen-coasting phase, in which the fireball expands as a shell of fixed radial width in its own local frame, with a width $\sim \bar{\gamma}_f R_i \sim \eta_i R_i$. Because of Lorentz contraction, the pulse

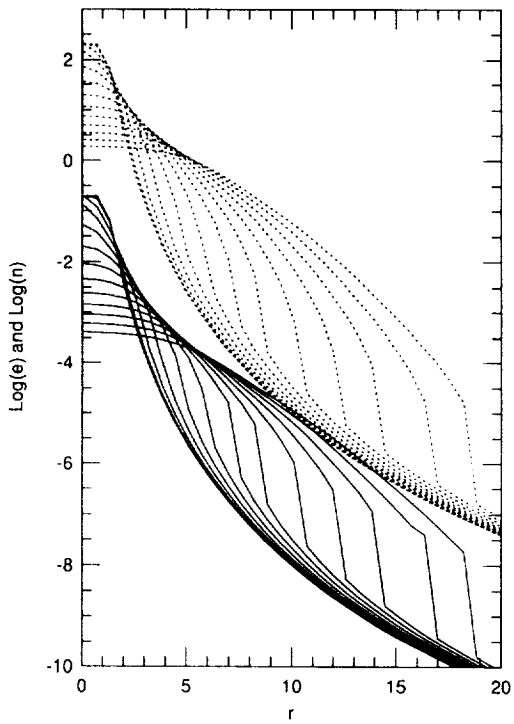

Figure 3. The energy density e (solid lines) and the mass density n (dotted lines) for a Newtonian or non-relativistic fireball with $\eta_i = 0.001$. Note that, while the final time is the same as in Fig. 1, the pulse has propagated a much shorter distance. There is no hint of a shell structure or a frozen-pulse shape here, in contrast to the relativistic case shown in Fig. 1.

appears to an observer to have a width of $\Delta r \approx R_i$. Eventually, the spread in $\overline{\gamma}_f$ as a function of radius within the fireball results in a spreading of the pulse and the fireball enters the coasting-expanding phase. In this final phase, $\Delta r \approx R_i t/\overline{\gamma}_f^2$, and the observed pulse width increases linearly with time.

The fireball can become optically thin in any of the above phases. Once this has happened the system ceases to behave like a fluid, and the radiation moves as a pulse with a constant width, while the baryons enter a coasting phase like the one described above. If the fireball becomes optically thin during the radiation-dominated phase, there will be a short photon-dragging phase, in which the baryons will continue to be accelerated by the radiation field until the mean free path for an electron is larger than the size of the fireball. The free-coasting phase for the baryons will begin from this point onwards.

We have verified many of these theoretical results by means of numerical simulations of spherically symmetric relativistic fireballs (Section 3). In particular, we confirm that the asymptotic solution with a frozen-pulse shape is reproduced to a good approximation. This is a very useful result, since it implies that in future it will not be necessary to carry out numerical simulations to very late times. As soon as the Lorentz factor of the expanding fluid reaches a moderately large value, say $\overline{\gamma} \sim 10$, we can use the theoretical results to extrapolate the pulse. This will provide a huge saving in computation time, particularly in cases where $\eta_i \gg 1$ and the asymptotic $\overline{\gamma}$ is very large.

An important aspect of fireball evolution that can be studied only by numerical simulations is the early stages of rearrangement. During this phase, the fireball is still only mildly relativistic, and it internally modifies the profiles of the energy and matter densities. From a number of simulations with different initial conditions, we find that the ratio of energy density to matter density, η, usually ends up with a lower value in the interior of the fireball than on the outside. The Lorentz factor γ also invariably increases from the inside out. These modified profiles enter the frozen-pulse phase and then do not change any further. Consequently, it appears to be a generic feature that any radiation that escapes from the fireball will be hot on the outside and cooler on the inside. In other words, the observed radiation pulse will tend always to have a spectral profile that shows a characteristic hard-to-soft transition as a function of time. This effect will be enhanced if the early radiation from the outside is emitted in the radiation-dominated phase and the later radiation from the interior is released from matter-dominated layers. The hard-to-soft signature will be even stronger in this case. Even if the radiation is not obtained directly from the fireball, but through shock reradiation as the fireball interacts with external matter, this feature should still be present.

The discussion in this paper has been restricted to general issues related to the evolution of relativistic fireballs, and we have focused on the phase in which the fireball expands effectively into a vacuum. The most immediate application of these results is to cosmological and Galactic halo models of gamma-ray bursts. Although these models differ in their explanations of the origin of the gamma-rays, all of them involve a stage in which the initially injected energy goes through a fireball phase. The scaling laws that we have written down for the matter and energy densities, the temperature and the Lorentz factor γ will therefore be relevant. Also, the hard-to-soft spectral evolution described above should be observed in each sub-burst, and possibly across the whole burst as well. In fact, this prediction is probably valid regardless of the way in which the final observed radiation is produced, whether it be through direct emission from the fireball when it becomes optically thin (Goodman 1986; Paczyński 1986; Shemi & Piran 1990) or through shock re-emission (Mészáros & Rees 1992, 1993).

ACKNOWLEDGMENTS

This work was supported by NASA grant NAG 5-1904 to Harvard University and by a BSF grant to the Hebrew University.

REFERENCES

Blandford R. D., McKee C. F., 1976, Phys. Fluids, 19, 1130
Blandford R. D., McKee C. F., 1977, MNRAS, 180, 343
Bowers R. L., Wilson J. R., 1991, Numerical Modeling in Applied Physics and Astrophysics. Jones and Bartlett, Boston
Cavallo G., Rees M. J., 1978, MNRAS, 183, 359
Goodman J., 1986, ApJ, 308, L47
Mészáros P., Rees M. J., 1992, MNRAS, 258, 41P
Mészáros P., Rees M. J., 1993, ApJ, 405, 278
Mészáros P., Laguna P., Rees M. J., 1993, ApJ, in press
Narayan R., Paczyński B., Piran T., 1992, ApJ, 395, L83
Paczyński B., 1986, ApJ, 308, L51
Paczyński B., 1990, ApJ, 363, 218
Piran T., Shemi T., 1993, ApJ, 403, L67
Shemi A., 1993, PhD thesis, Tel Aviv University
Shemi A., Piran T., 1990, ApJ, 365, L55
Vitello P., Salvati M., 1976, Phys. Fluids, 19, 1523
Weinberg S., 1973, Gravitation and Cosmology. Wiley, New York